Rab GTPase–Myo5B complexes control membrane recycling and epithelial polarization

Joseph T. Roland[a,1], David M. Bryant[b,1], Anirban Datta[b], Aymelt Itzen[c], Keith E. Mostov[b], and James R. Goldenring[a,2]

[a]Departments of Surgery and Cell and Developmental Biology, Epithelial Biology Center, Vanderbilt University School of Medicine and the Nashville Veterans Affairs Medical Center Nashville, TN 37232; [b]Department of Anatomy, University of California, San Francisco, CA 94143; and [c]Department of Physical Biochemistry, Max-Planck-Institute of Molecular Physiology, D-44227 Dortmund, Germany

Edited* by David D. Sabatini, New York University School of Medicine, New York, NY, and approved December 30, 2010 (received for review July 22, 2010)

The Rab GTPases are the largest family of proteins regulating membrane traffic. Rab proteins form a nidus for the assembly of multiprotein complexes on distinct vesicle membranes to regulate particular membrane trafficking pathways. Recent investigations have demonstrated that Myosin Vb (Myo5B) is an effector for Rab8a, Rab10, and Rab11a, all of which are implicated in regulating different pathways for recycling of proteins to the plasma membrane. It remains unclear how specific interactions of Myo5B with individual Rab proteins can lead to specificity in the regulation of alternate trafficking pathways. We examined the relative contributions of Rab/Myo5B interactions with specific pathways using Myo5B mutants lacking binding to either Rab11a or Rab8a. Myo5B Q1300L and Y1307C mutations abolished Rab8a association, whereas Myo5B Y1714E and Q1748R mutations uncoupled association with Rab11a. Expression of Myo5B tails containing these mutants demonstrated that Rab11a, but not Rab8a, was required for recycling of transferrin in nonpolarized cells. In contrast, in polarized epithelial cyst cultures, Myo5B was required for apical membrane trafficking and de novo lumen formation, dependent on association with both Rab8a and Rab11a. These data demonstrate that different combinations of Rab GTPase association with Myo5B control distinct membrane trafficking pathways.

Recycling to the plasma membrane of proteins internalized by either clathrin-dependent or clathrin-independent endocytosis requires the coordinated action of Rab small GTPases and class V myosin motors (Myo5; ref. 1). Three mammalian isoforms of Myo5 motors exist: Myo5A, Myo5B, and Myo5C (2). Myo5 motors function in multiple trafficking pathways through association with several different Rab GTPases (3, 4). For instance, Rab11a interacts with Myo5A and Myo5B, whereas Rab8a can associate with all three Myo5 isoforms (4). Splice variations in Myo5 motors control some Rab associations, such as Myo5A and Myo5B interaction with Rab10 only when Exon D is present (4). In addition, Myo5 motors may bind directly to Rabs, or indirectly through Rab effectors (5), increasing the complexity of motor association with membrane trafficking systems. However, it remains unclear whether Rab proteins use Myo5 motors in distinct vesicle trafficking pathways or, alternatively, whether associations with Myo5 coordinate Rab proteins in the sequential regulation of different aspects of individual trafficking pathways.

A number of investigations over the past several years have implicated Myo5B in the regulation of membrane protein recycling to plasma membrane surfaces. However, the roles of Myo5B and its associated Rab proteins differ in nonpolarized and polarized cells. In nonpolarized cells, Myo5B regulates general membrane recycling dependent on Rab11a, as exemplified by the recycling of the transferrin receptor (6). In contrast, in polarized cells, Rab11a and Myo5B no longer regulate transferrin-receptor recycling, but instead function in pathways leading to the apical membrane, including basolateral–apical transcytosis and apical recycling (6). In polarized cells, basolateral recycling of the transferrin receptor is not dependent on Rab11a or Myo5B.

Recent investigations have also implicated Myo5B in the establishment of polarized function in epithelial cells. Indeed, loss-of-function Myo5B mutations underlie neonatal diarrheal disease in children with microvillus inclusion disease (MVID), likely due to defects in apical polarization and transporter protein localization (7). Moreover, Myo5B functions in apical secretion and lumen morphogenesis during formation of the *Drosophila* photoreceptors and tracheal system (8, 9). Similarly, both Rab11a and Rab8a have been implicated in establishing epithelial polarity. De novo lumen formation in 3D epithelial cyst cultures requires the trafficking of apical polarity proteins (such as Par3) and luminal proteins (such as the sialomucin podocalyxin). These apical trafficking programs are controlled by Rab11a, which recruits and activates Rab8a on subapical vesicles via the Rab GEF, Rabin8 (10). In addition, phosphorylation by Par1b of Rab11-FIP2, which binds to both Rab11a and Myo5B, is necessary for proper establishment of polarity in Madine–Darby canine kidney (MDCK) cells (11). The cooperation of Rab8a and Rab11a in apical trafficking supports the hypothesis that association with both GTPases may regulate Myo5B participation in apical membrane transport.

We now have used mutants of Myo5B to ascertain the relative contributions of Rab8a, Rab10, and Rab11a to Myo5B-dependent transport processes. In nonpolarized HeLa cells, Myo5B regulated transferrin receptor recycling dependent on Rab11a, but not recycling dependent on Rab8a. In contrast, in polarized MDCK cysts, Myo5B was required for apical polarization and lumen formation dependent on interactions with both Rab8a and Rab11a. These results demonstrate that although association of a single Rab protein with Myo5B can regulate simple recycling pathways, the interaction of Myo5B with multiple Rab proteins is required for the more complex processes involved in the establishment of apical polarity in epithelial cells.

Results

Identification of Rab11-Specific Mutations in Myo5B Tail. Rab8a, Rab10, and Rab11a interact with Myo5B in nonoverlapping regions of its carboxyl-terminal tail (3, 4, 6, 12). Thus, we reasoned that we could identify mutations in Myo5B that differentially inhibited binding of each Rab. In these studies, we excluded Rab10 binding by using the Myo5B splice variant lacking Exon D/Exon 31 (Myo5BΔD), which is required for Rab10 association (4). Lipatova et al. (13) identified mutations in the yeast class V Myosin motor, Myo2p, which inhibited interaction with Ypt31p/Ypt32p, members of the Rab11 GTPase family. Two of these mutated residues, Y1415 and Q1447, are highly conserved in human Myo5A and Myo5B, but not Myo5C (residues Y1714 and Q1748 in Myo5B, Fig. 1*A*). To determine whether these residues are similarly important for Rab11a-Myo5B association, we ex-

Author contributions: J.T.R., D.M.B., A.I., K.E.M., and J.R.G. designed research; J.T.R., D.M.B., A.D., and A.I. performed research; J.T.R., D.M.B., and A.I. contributed new reagents/analytic tools; J.T.R., D.M.B., A.D., A.I., and J.R.G. analyzed data; and J.T.R., D.M.B., A.I., K.E.M., and J.R.G. wrote the paper.

The authors declare no conflict of interest.

*This Direct Submission article had a prearranged editor.

[1]J.T.R. and D.M.B. contributed equally to this work.

[2]To whom correspondence should be addressed. E-mail: jim.goldenring@vanderbilt.edu.

This article contains supporting information online at www.pnas.org/lookup/suppl/doi:10.1073/pnas.1010754108/-/DCSupplemental.

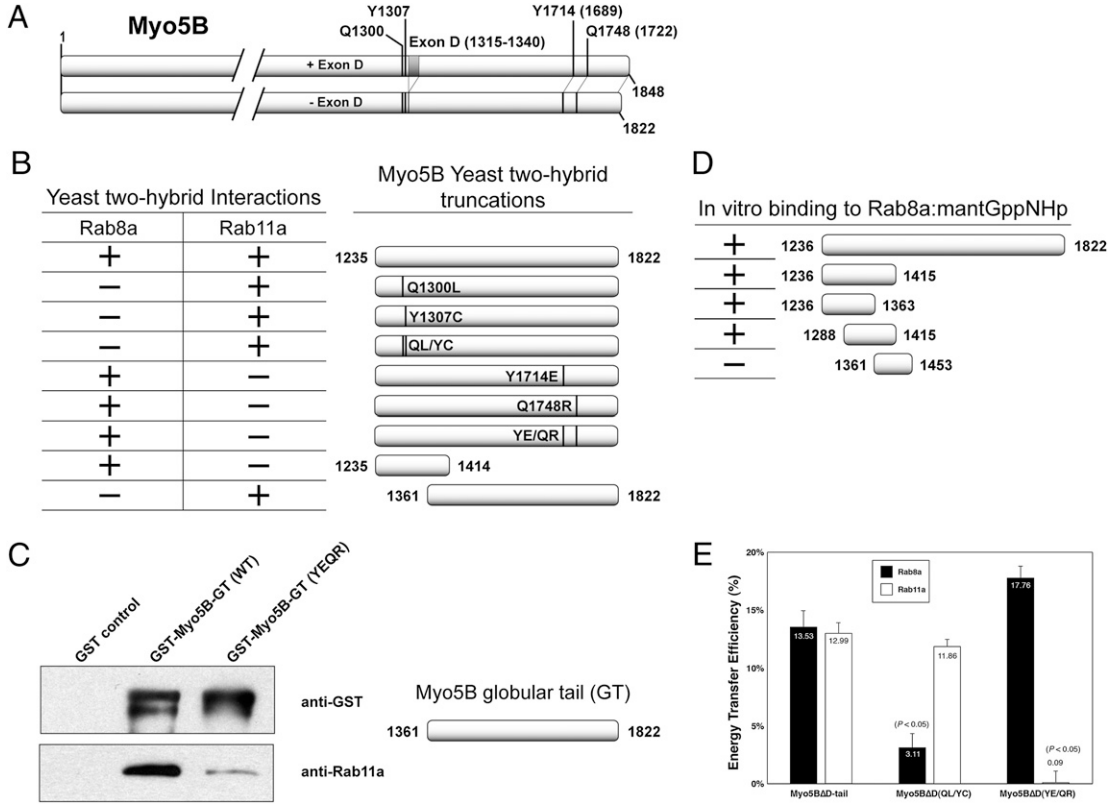

Fig. 1. Identification of Rab8a- and Rab11a-specific mutations in Myo5B. (*A*) Schematic representation of Myo5B. (*Upper*) Myo5B including Exon D (+D, amino acids 1315–1340). (*Lower*) The splice variant lacking Exon D (ΔD). The locations of the mutations detailed in this study are represented: Q1300, Y1307, Y1714, and Q1748. (*B*) Yeast two-hybrid assays were performed with plasmids encoding the DNA binding domain of GAL4 fused to Rab8a or Rab11a versus the activation domain of GAL4 fused to different Myo5B tail constructs. Positive and negative colonies were identified as described in *Materials and Methods*. Two mutations, Q1300L and Y1307C, alone or together disrupt interaction with Rab8a, but not Rab11a. Conversely, mutations Y1714E and Q1748R, alone or together, disturb interaction with Rab11a, but not Rab8a. In addition, the N terminus of Myo5B tail (amino acids 1235–1414) is sufficient to bind Rab8a, but not Rab11a. (*C*) The globular tail (GT) of Myo5B and Rab11a bind directly in vitro. Western blot analysis of GST pull-down experiments reveals that Rab11a directly associates with amino acids 1361–1822 of Myo5B. Double mutation of this domain at residues 1714 and 1748 dramatically lowered the ability of Rab11a to copurify with Myo5B (1361-1822). (*D*) Characterization of the direct interaction of Myo5B with Rab8:mantGppNHp. Examination of interactions of recombinant truncations of Myo5B (1288-1441) with recombinant Rab8 loaded with mantGppNHp in a stopped flow analysis revealed direct binding of Rab8a between amino acids 1288 and 1363 of Myo5B. (*E*) Rab8a- and Rab11a-specific mutations in Myo5BΔD tail block FRET. FRET microscopy was performed on HeLa cells cotransfected with mCerulean-tagged Myo5BΔD tail constructs (WT, QL/YC, or YE/QR) and mVenus-tagged Rab8a or Rab11a. Energy transfer efficiency was calculated by measuring the fluorescence intensity of a photobleached region of interest (ROI) before (pre) and after (post) photobleaching. Error bars indicate the SEM. Rab8a-specific mutations (Q1300L/Y1307C) blocked the ability of Myo5BΔD tail to efficiently FRET with Rab8a, whereas the Rab11a-specific mutations (Y1714E/Q1748R) inhibited FRET with Rab11a.

amined the Myo5B tail containing these mutations for Rab8a and Rab11a association in a yeast two-hybrid assay. Although wild-type Myo5B tail interacted with both Rab8a and Rab11a, mutation of either of these two residues abolished Rab11a, but not Rab8a, association (Fig. 1*B*). Thus, the Rab11 binding domain of Myo5B is conserved from yeast to human, is distinct from the Rab8a binding region, and requires residues Y1714 and Q1748 in the distal part of the globular Myo5B tail.

Establishment of direct binding of Rab proteins with Myo5B, as opposed to interaction through intervening adaptor proteins, has been controversial. Indeed, whereas genetic and FRET imaging studies have supported direct association of Rab11a with Myo5B, previous studies have been unable to establish in vitro reconstitution of the Myo5B interaction with Rab11a (6). Therefore, as an alternative approach, we coexpressed His-tagged Rab11a and GST-tagged Myo5B globular tail [GST-Myo5B-GT (WT)] or Myo5B-GT containing both mutations associated with abolished Rab11a by yeast two-hybrid assays [GST-Myo5B-GT (YE/QR)] in bacteria. Notably, recombinant Rab11a copurified with wild-type Myo5B-GT, whereas binding was greatly reduced with the YE/QR mutant (81.6% ± 5.8% reduction; Fig. 1*C*). These results indicate that Rab11a can bind directly to Myo5B in vitro, and that this interaction requires residues Y1714 and Q1748.

Determination of the Rab8a Binding Domain of Myo5B. We have previously noted the association of Rab8a within a short region of Myo5B tail containing alternatively spliced exons ABCE (amino acids 1236–1822; ref. 4). To define more precisely this association domain, we loaded recombinant Rab8a with the nonhydrolyzable GTP analog mantGppNHp and examined in vitro binding to progressive recombinant truncation fragments of the Myo5B tail. These studies narrowed the Rab8a-interacting region to a 75-aa stretch (1288–1363; Fig. 1*D*). Analysis of the interaction of Rab8a with Myo5B (1288–1441) in a stopped-flow assay showed a linear dependence of the observed rate constant on Myo5B fragment concentration for interaction with mantGppNHp-loaded Rab8a (Fig. S1 *A* and *B*). The determination of the association and dissociation rate constants (Fig. S1*B*) led to a K_d of 11 μM. Thus, GTP-Rab8a, similar to Rab11a, can interact directly with Myo5B in vitro, verifying Myo5B as a bona fide direct Rab8a effector.

To generate mutants of Myo5B that are unable to bind Rab8a, the tail of Myo5B was subjected to random mutagenic PCR, and the resulting sequences were screened for their ability to interact

with either Rab8a or Rab11a in yeast two-hybrid assays. Two point mutations were identified that abolished Rab8a interaction, but maintained Rab11a association. These mutations in the Myo5B tail were located within 7 aa of each other at Q1300L and Y1307C (Fig. 1*B*) in Exon C/Exon 30, notably within the small fragment reported to interact with Rab8a (4).

FRET Between Rab8a or Rab11a and Mutant Myo5B Tails. To examine whether point mutations in Myo5B, which altered interactions with Rab8a or Rab11a *in vitro,* elicited similar effects in vivo, we performed FRET analysis between either Rab8a or Rab11a and the Myo5BΔD tail (14). As reported (4), FRET was observed between wild-type mCerulean-Myo5BΔD tail and either mVenus-Rab8a or mVenus-Rab11a (Fig. 1*E*), confirming our in vitro data. In cells coexpressing the Myo5BΔD(QL/YC) tail (unable to bind Rab8a in vitro) FRET with Rab8a, but not with Rab11a, was significantly reduced. Also confirming the in vitro data, no FRET was observed between the Myo5BΔD(YE/QR) tail and Rab11a, but FRET with Rab8a was maintained. These results verify uncoupling of Myo5B mutants from specific interactions with either Rab8a or Rab11a in vivo.

Mutations in Myo5B Independently Affect Localization of Either Rab8a or Rab11a. In nonpolarized HeLa cells, expression of the motorless tail of Myo5B causes the collapse of the plasma membrane recycling systems containing Rab8a and Rab11a into perinuclear cisternae, without affecting endolysosomal (Rab5/Rab4/Rab7-containing) or Golgi apparatus membranes (3, 6). We used these functional assays to test the effects of mutations in Myo5B on the recycling system of HeLa cells. Accordingly, in cells expressing the EGFP-Myo5BΔD tail, both Rab8a and Rab11a were mislocalized to Myo5BΔD tail-containing collapsed membrane cisternae (Fig. 2 *A* and *D*) compared with their endogenous localization (Fig. S2), as were the Myo5B-dependent cargoes transferrin and MHC class I (Fig. 2 *G* and *J*). Notably, Myo5BΔD(QL/YC) tail expression failed to alter Rab8a localization (Fig. 2*B*), although it still sequestered Rab11a (Fig. 2*E*). Conversely, Myo5BΔD(YE/QR) tail expression mislocalized Rab8a to perinuclear cisternae (Fig. 2*C*), whereas Rab11a localization was unaffected (Fig. 2*F*). These data confirm that the QL/YC and YE/QR mutations functionally uncouple Myo5B from Rab8a and Rab11a pathways, respectively, in vivo.

Confirming that uncoupling of these Rab–Myo5B interactions affected cargo-specific transport pathways, we observed that, similar to wild-type Myo5BΔD tail, Myo5BΔD(QL/YC) tail, but not the Myo5BΔD(YE/QR) tail, perturbed transferrin recycling in nonpolarized HeLa cells (Fig. 2 *H* and *I*). These findings are consistent with a Rab11a-dependent process (15). Interestingly, the Myo5BΔD(QL/YC) tail retained some ability to cause sequestration of recycling MHC class I molecules in perinuclear cisternae (Fig. 2*K*), albeit to a lower extent than wild-type Myo5B tail (91.5% ± 2.2% vs. 83.5% ± 3.6% colocalization), suggesting that Rab11a association participates in Myo5B tail-induced inhibition of MHC class I recycling. Importantly, we observed that expression of the Myo5BΔD(YE/QR) tail was unable to affect MHC class I recycling (Fig. 2*L*), supporting the role for Rab8a in MHC recycling. Together, these results suggest that the Rab11a-dependent loading of Myo5B onto vesicles is crucial for membrane recycling of both clathrin-dependent and clathrin-independent cargoes in nonpolarized cells.

Myo5B Participates in Rab8a- and Rab11a-Dependent Apical Transport Pathways. In polarized epithelial cells, Rab11a and Rab8a subsume roles more specific to trafficking to the apical membrane (16). Therefore, we examined the dependence of Myo5B on interaction with Rab8a or Rab11a in polarized cells using 3D MDCK cyst cultures. When MDCK cells are grown in extracellular matrix-containing culture conditions, they undergo morphogenesis to form cystic structures: a spherical monolayer of cells surrounding a central lumen, more faithfully modeling the in vivo architecture than traditional 2D monolayer culture

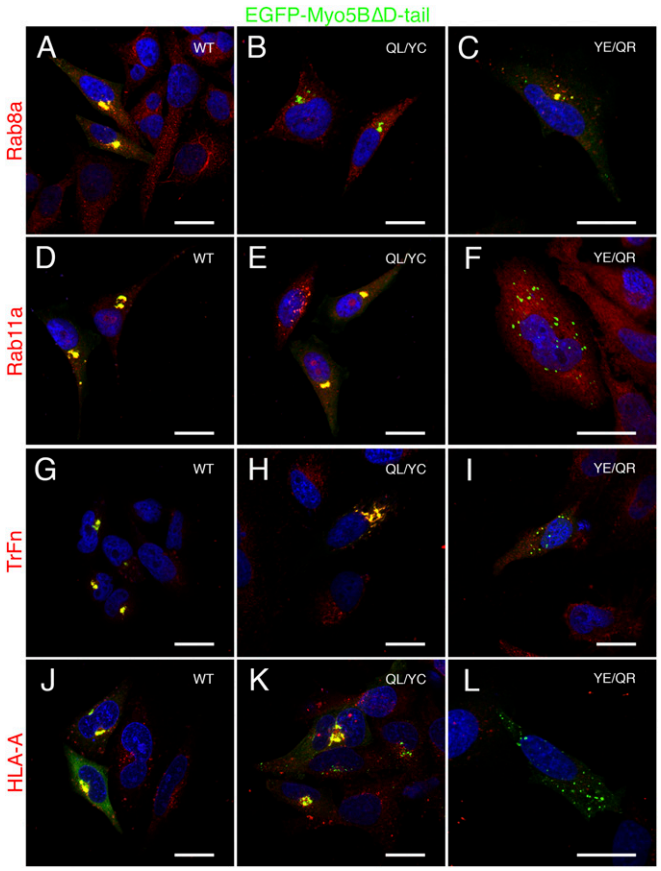

Fig. 2. Mutations in Myo5B tail independently disrupt interaction with Rab8a or Rab11a and recycling of transferrin and MHC class I. Endogenous Rab8a is mislocalized to Myo5BΔD tail-induced perinuclear cisternae in transfected HeLa cells expressing the dominant-negative GFP-fusion protein (*A*). The Rab8-uncoupled (QL/YC) mutant tail no longer accumulates Rab8a (red) (*B*), whereas the Rab11a-uncoupled tail (YE/QR) still accumulates Rab8a (*C*). (*D*) Similarly, endogenous Rab11a was localized to Myo5BΔD tail-induced cisternae. Converse to the pattern observed for Rab8a, the QL/YC mutant tail (*E*), but not the YE/QR (*F*) accumulated Rab11a. (*G*) Expression of Myo5BΔD tail inhibited the recycling of Alexa-568-labeled transferrin in HeLa cells. Internalized transferrin was sequestered in Myo5BΔD tail-positive perinuclear cisternae following a pulse–chase (50-min pulse; 60-min chase). (*H*) The Rab8a-uncoupled QL/YC tail still sequestered internalized transferrin, due to the continued ability to interact with Rab11a. In contrast, the Rab11a-uncoupled tail (YE/QR) failed to accumulation transferrin (*I*). MHC class I molecules (HLA-A) were internalized in the presence of a specific monoclonal antibody (W6/32), and visualized by counter staining with Alexa-568-labeled anti-mouse antibodies. As with transferrin, MHC class I molecules were retained with wild-type (*J*) and Rab8a-uncoupled (QL/YC; *K*) Myo5BΔD tails, but not the Rab11a-uncoupled (YE/QR) Myo5B tail (*L*). This result suggests that Rab11a-mediated loading of Myo5B onto membranes, in a step upstream of Rab8a interaction, may be required for proper function. (Scale bars: 20 μm.)

(17, 18). De novo generation of the apical lumen requires Rab8a- and Rab11a-dependent transport of the apical membrane resident protein podocalyxin/gp135 (PCX; ref. 19) to regions between neighboring cells to initiate lumen formation (10, 20).

In control MDCK cysts, PCX localized exclusively to the apical, luminal membrane (Fig. 3*Aa*). However, stable expression of an EGFP-Myo5BΔD tail induced the appearance of subapical collapsed cisternae containing a pool of PCX (Fig. 3*Ab*, arrowheads), without disrupting lumen formation. In contrast with the wild-type tail, the Myo5BΔD(QL/YC) tail failed to accumulate PCX intracellularly or induce the subapical cisternae, instead localizing to vesicles across the entire subapical region (Fig. 3*Ac*, arrows). Notably, the Myo5BΔD(YE/QR) tail largely localized to the cytoplasm and to a lesser extent under the

CELL BIOLOGY

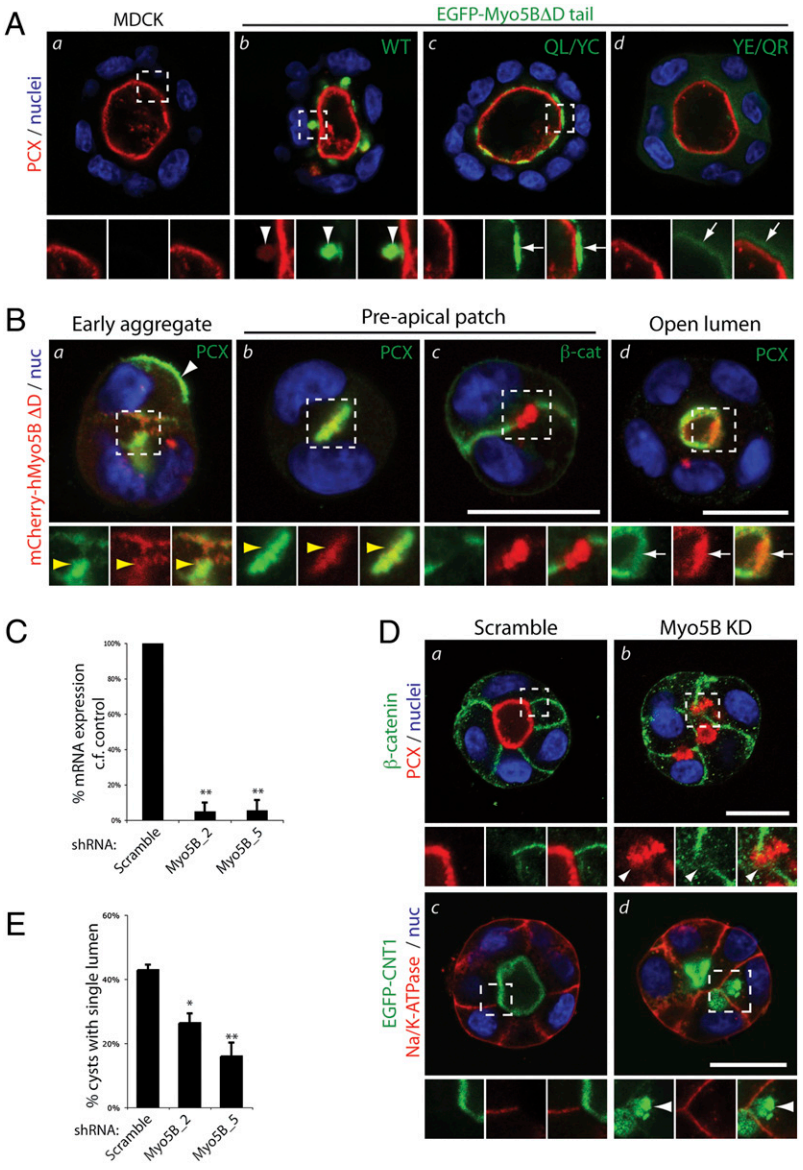

Fig. 3. Myo5B participates in apical traffic and de novo lumen formation. (*A*) 72h MDCK (*a*) and MDCK EGFP-Myo5BΔD tail (WT, *b*; QL/YC, *c*; YE/QR, *d*) cysts were costained for nuclei (blue) and PCX (red). Note that the Myo5BΔD tail WT, but not the two mutants, accumulates a pool of PCX in subapical cisternae. Arrowheads, coaccumulation of PCX and EGFP-Myo5BΔD tail in subapical cisternae. Arrows, subapical EGFP-Myo5BΔD tail fragments without PCX labeling. (*B*) Localization of mCherry-Myo5BΔD during cyst lumen formation. MDCK mCherry-Myo5BΔD (red) cysts grown for 12–48 h and imaged at different stages of cyst development were stained for nuclei (blue) and either PCX (*a*, *b*, and *d*) or β-cat (β-catenin; *c*; both green). White arrowheads, peripheral PCX; white arrows, mCherry-Myo5BΔD. Note colocalization of PCX and mCherry-Myo5B on intracellular vesicles (*a*) and the Preapical patch (yellow arrowheads; *b*), but not β-catenin-positive junctions (*c*), before mCherry-Myo5BΔD becomes concentrated underneath the luminal surface (white arrows), once lumens have formed (*d*). (*C*) Knock down of endogenous Myo5B expression. Stable Myo5B KD in cells expressing control (scramble) Myo5B shRNAs (Myo5B_2, Myo5B_5) was verified by qRT-PCR and normalized to GAPDH expression. Values are mean ± SD from three replicates. $^{**}P < 0.001$. (*D*) Myo5B is required for lumen formation. MDCK (*a* and *b*) or MDCK EGFP-CNT1 (*c* and *d*; green) cysts expressing stable shRNAs (control, Myo5B KD [Myo5B_5]) grown for 48 h were labeled for nuclei (blue) and either PCX (red; *Upper*) and β-cat (green; *Upper*) or Na/K-ATPase (red; *Lower*). Arrowheads denote intracellular accumulation of apical, but not basolateral, cargo upon Myo5B KD. (*E*) Myo5B is required for lumen formation. Cysts (48 h) expressing stable RNAi (Control, Myo5B_2, Myo5B_5) were scored for single lumen formation. Values are mean ± SD from three replicates. $n \geq 100$ cysts/replicate. $^{*}P < 0.05$; $^{**}P < 0.001$. (*A Lower*, *B Lower*, and *D Lower*) Higher magnification, split-color images of regions boxed above. (Scale bar: 20 μm.)

luminal membrane, also failing to accumulate a pool of PCX intracellularly (Fig. 3*Ad*). These data reveal that in polarized epithelial cells, interaction with Rab11a is required for proper targeting of the Myo5B tail to subapical endosomes. Furthermore, in contrast with membrane recycling in nonpolarized cells, association of Myo5B with Rab8a is required for apical transport processes involving PCX.

Lumen Formation Requires Both Rab8a–Myo5B and Rab11a–Myo5B Interactions. We next examined whether Myo5B participates in de novo lumen formation. During MDCK cyst lumen formation, PCX transcytoses from the periphery of early two-cell aggregates to the nascent central lumen via Rab8a- and Rab11a-positive vesicles (10). In MDCK cysts undergoing initial stages of de novo lumen generation, PCX was found at the cyst periphery (Fig. 3*Ba*, white arrowhead) and in vesicles close to the apical membrane initiation site (10), which was colabeled for full-length mCherry-Myo5BΔD (Fig. 3*Ba*, yellow arrowheads). The mCherry-Myo5BΔD overlapped with PCX at the preapical patch (ref. 20; Fig. 3*Bb*), a luminal domain precursor consisting of a nonexpanded luminal space with closely opposed membranes, but devoid of cell–cell junctions (β-catenin; Fig. 3*Bb*). Once lumens had formed, mCherry-Myo5BΔD localized to subapical vesicles (Fig. 3*Bd*). Because Myo5BΔD does not interact with Rab10, these data suggest that Rab8a or Rab11a may control the targeting of Myo5B to apically destined vesicles participating in de novo establishment of apical polarity.

We next examined a potential requirement for Myo5B in lumen generation. Because expression of the Myo5B tail fragment did not disrupt lumen formation, we stably depleted endogenous Myo5B via lentiviral shRNA. Two different shRNA plasmids efficiently removed the majority of Myo5B mRNA (Myo5B_2, Myo5B_5; Fig. 3*C*). In contrast to control cysts with a clear segregation between apical proteins at the lumen (PCX, GFP-CNT1; Fig. 3*D a* and *c*) and basolateral cargoes (β-catenin, Na/K-ATPase; Fig. 3*D b* and *d*), depletion of Myo5B resulted in apical, but not basolateral, cargo accumulation in intracellular vesicles close to the cell surface (Fig. 3*Dd*, arrowheads). Accordingly, Myo5B knockdown significantly disrupted the ability of cysts to form a single lumen (Fig. 3*E*). Similar disruption to PCX, GFP-CNT1 and lumen formation are observed upon Rab8a or Rab11a knockdown (10). Thus, Myo5B plays a critical role in the plasma membrane delivery of vesicles involved in de novo lumen formation.

The foregoing data suggest that Myo5B associates with subapical endosomes via Rab11a, but that subsequent apical transport processes require Rab8a–Myo5B interactions. To confirm this,

we examined de novo lumen formation in cysts with endogenous Myo5B knockdown, reconstituted with mCherry-tagged human, RNAi-resistant Myo5B full-length variants. Coexpression of scrambled shRNA in MDCK with each mCherry-Myo5BΔD protein (wild type, QL/YC, YE/QR; Fig. 4*A b–d* and *B*) did not affect PCX localization or lumen formation, suggesting that these Myo5B constructs are not dominant over endogenous protein in cyst cultures. As expected, endogenous Myo5B knockdown resulted in intracellular PCX accumulation (Fig. 4*Ae*) and decreased single lumen formation (Fig. 4*B*), compared with control cysts with a single lumen decorated by PCX (Fig. 4*A a* and *B*). Expression of mCherry-Myo5BΔD wild type, which localized to subapical vesicles in all instances (Fig. 4*A b* and *f*, arrowheads), restored luminal targeting of PCX and lumen formation in the context of endogenous Myo5B depletion (Fig. 4*A f* and *B*). Similar to expression of the Myo5BΔD tail fragments, mCherry-Myo5BΔD(QL/YC) targeted to subapical vesicles, likely reflecting maintained binding to Rab11a (Fig. 4*A c* and *g,* arrows). Cherry-Myo5BΔD(YE/QR) mainly localized to the cytoplasm with a pool of faint subapical labeling (Fig. 4*A d* and *h*, arrows), also mirroring expression of its cognate tail fragment. Unlike mCherry-Myo5BΔD wild type, however, expression of mCherry-Myo5BΔD mutants deficient in either Rab8a (QL/YC; Fig. 4*Ag*) or Rab11a (YE/QR; Fig. 4*Ah*) binding were unable to rescue single lumen formation upon endogenous Myo5B depletion. Notably, the mCherry-Myo5B+D splice variant (which also binds Rab10) similarly localized to subapical vesicles (Fig. S3*B*, arrows), but was unable to rescue lumen formation upon depletion of endogenous Myo5B, instead decreasing lumen formation even in scrambled-shRNA expressing cells (Fig. S3 *B* and *C*). These data confirm that, although Rab11a association is required for proper targeting of full length Myo5B to subapical vesicles, Myo5B must additionally associate with Rab8a, but not Rab10, to ensure correct apical vesicle delivery and polarization during de novo lumen formation.

Discussion

Our findings indicate that different Rab-Myo5B associations may occur during membrane transport in nonpolarized or polarized cells. Using a combination of splice variants and point mutations in Myo5B, we identified specific Myo5B-dependent pathways with exclusive and nonexclusive dependence on Rab8a, Rab10, or Rab11a. Transferrin trafficking in nonpolarized HeLa cells was affected by perturbing Rab11a-Myo5B, but not Rab8a–Myo5B function, confirming previous results (4). In contrast, although MHC Class I trafficking has been reported as Rab8a-dependent (21), our data indicate an additional role for Rab11a. Moreover, in polarized epithelial cysts Myo5B interaction with both Rab8 and Rab11a, but not Rab10, was required for proper PCX trafficking and de novo lumen formation. In these polarized cells, Rab11a association was required for proper localization of Myo5B to subapical endosomes, which may then facilitate Rab8a–Myo5B interactions. Notably, Rab11a induces Rab8a activation on subapical vesicles by recruiting a Rab8 GEF, Rabin8, during ciliogenesis (22), and de novo lumen formation (10), suggesting that a Rab11a-to-Rab8a cascade may be a common feature of apical trafficking pathways. As Rab8a and Rab11a bind in different regions of Myo5B, it will be of interest to determine in the future whether simultaneous or sequential Rab binding regulates Myo5B function.

Previous investigations have indicated a role Myo5B in apical membrane regulation of polarized epithelia. Expression of the Myo5B tail inhibits bile canaliculus formation in hepatocytes in culture (23). These studies used a Myo5B tail construct including exon D, which potentially inhibits Rab8a, Rab10, and Rab11a (4). Using knockdown and re-expression strategies in our system, lumen formation required Myo5B association with Rab8a- and Rab11a-dependent trafficking pathways, but was perturbed by Myo5B variants that conferred Rab10 association. These findings are supported by our observations that Myo5BΔD, which does not bind Rab10, is the predominant splice form in kidney

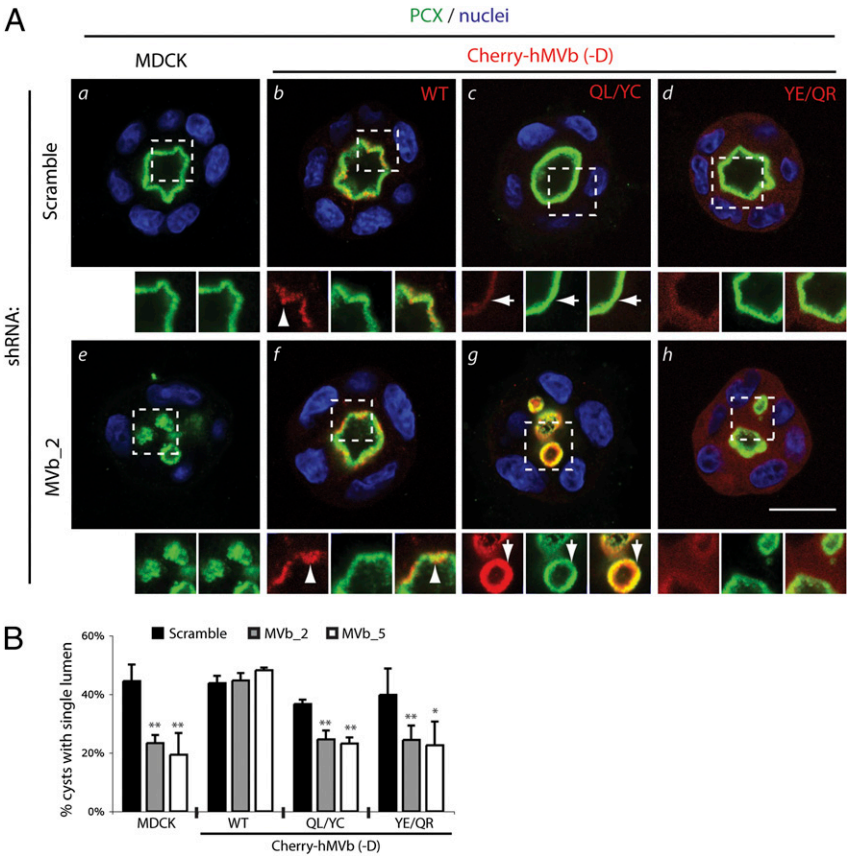

Fig. 4. Both Rab8a-Myo5B and Rab11a-Myo5B interactions are required for apical lumen formation. (*A*) Rab-dependency of Myo5B during lumen formation. Cysts (48 h) from MDCK (*a* and *e*) or MDCK expressing mCherry-Myo5BΔD (*b* and *f*), mCherry-Myo5BΔD(QL/YC) (*c* and *g*), mCherry-Myo5BΔD(YE/QR) (*d* and *h*), coexpressing scrambled (*a-d*) or Myo5B shRNA (Myo5B_2; *e–h*) were stained for PCX (green) and nuclei (blue). Arrowhead denotes subapical vesicular Myo5B labeling; arrows denote Myo5B labeling closely apposed to the lumen. Note the reduced vesicular and increased cytoplasmic fluorescence for the YE/QR mutant. (*Lower*) Higher magnification, split-color images of regions boxed above. (*B*) Quantitation of single lumen formation. Graph denotes the percentage of cysts forming a single lumen in 48-h MDCK, MDCK mCherry-Myo5BΔD, MDCK mCherry-Myo5BΔD (QL/YC), or MDCK mCherry-Myo5BΔD(YE/QR) cysts, expressing scrambled or two different Myo5B shRNAs (Myo5B_2, Myo5B_5). Values are mean ± SD from three replicates. $n \geq 100$ cysts per replicate. Significance is calculated in reference to control MDCK lumen formation in cysts expressing scramble shRNA. $^{*}P < 0.05$; $^{**}P < 0.001$. (Scale bar: 20 μm.)

(4). The precise function of Rab10 association with Myo5B remains to be elucidated. Myo5B can also associate with Rab25 through the same binding site used by Rab11a (6). Recent investigations indicate that Rab25 regulates apical to basal transcytosis (24) and 3D cyst lumen formation (10) in MDCK cells. Although Rab25-deficient mice show no appreciable kidney or intestinal phenotype, breeding of either Apc^{Min} or $Smad3^{+/-}$ mice onto a $Rab25^{-/-}$ background promotes intestinal tumorigenesis (25). Thus, the contribution of Rab25–Myo5B interactions to epithelial polarization remains to be determined.

Myo5B-inactivating mutations, either point mutations or truncations, are responsible for the genesis of MVID, which causes severe neonatal diarrhea due to a prominent loss of apical microvilli in intestinal epithelial cells (7, 26). Although no mutations in Rab8a been identified in MVID patients, this general intestinal cell phenotype is in part recapitulated in Rab8a knockout mice (27). Interestingly, although we have observed aberrant subapical vesicular cisternae in MDCK cells expressing the Myo5B tail fragment, these membranes differ from the apical inclusions seen in the MVID patients, as they are devoid of an F-actin/ezrin-containing coat. Thus, a strict requirement of Rab8a–Myo5B function in apical trafficking pathways may differ among epithelial tissues, or alternately kidney epithelia in vivo may have more adaptive mechanisms to compensate for loss of Myo5B function.

Knockdown of Myo5B, but not tail fragment expression, impaired normal apical polarization. In contrast, in MDCK cell monolayers grown on filters, the Myo5B tail inhibits Myo5B-dependent basal to apical transcytosis and apical recycling (6). It is important to note that such monolayer assays examine acute inhibition of Myo5B-dependent pathways (i.e., over short periods, <2 h), whereas examination of lumen formation is a test of chronic inhibition (48-72 h). Thus, cells in 3D culture, similar to in vivo, may compensate for such loss-of-function alleles. Accordingly, the non-Rab-binding full-length Myo5B mutants only perturbed lumen formation when endogenous Myo5B was depleted. These findings underscore the importance of combined RNAi and loss-of-function approaches in the analysis of membrane transport during epithelial polarization.

Taken together, we demonstrate here that Myo5B is critical for the early stages of epithelial cell polarization during de novo lumen formation and that Rab11a association is crucial for targeting Myo5B to recycling vesicles. Furthermore, we demonstrate that specific utilization of some Rabs (Rab8a, Rab11a), and the exclusion of others (Rab10), by Myo5B regulates the function of specific membrane trafficking pathways. Thus, differential utilization of particular Myo5B-Rab complexes may provide for specialization among membrane recycling and apical polarization pathways.

Materials and Methods

For a description of the materials and methods utilized for antibodies, 2D cell culture and immunocytochemistry, 3D cell culture, mutagenesis, yeast two-hybrid assays, bacterial protein production and purification, determination of Rab8a/MyoVB interactions, statistics, RNAi, recycling assays, and FRET, see *SI Text*.

ACKNOWLEDGMENTS. Confocal images were generated through the use of the Vanderbilt University Medical Center Cell Imaging Shared Resource (supported by National Institutes of Health Grants CA68485, DK20593, DK58404, HD15052, DK59637, and EY08126). This work was supported by National Institutes of Health Grants R01 DK070856 and R01 DK48370 (to J.R.G.); R01 DK074398, R37 AI25144, and P01 AI53194 (to K.E.M.); and F32 DK072789 (to J.T.R). D.M.B. is a Susan G. Komen Postdoctoral Fellow.

1. Rodriguez-Boulan E, Kreitzer G, Müsch A (2005) Organization of vesicular trafficking in epithelia. *Nat Rev Mol Cell Biol* 6:233–247.
2. Rodriguez OC, Cheney RE (2002) Human myosin-Vc is a novel class V myosin expressed in epithelial cells. *J Cell Sci* 115:991–1004.
3. Roland JT, Kenworthy AK, Peranen J, Caplan S, Goldenring JR (2007) Myosin Vb interacts with Rab8a on a tubular network containing EHD1 and EHD3. *Mol Biol Cell* 18:2828–2837.
4. Roland JT, Lapierre LA, Goldenring JR (2009) Alternative splicing in class V myosins determines association with Rab10. *J Biol Chem* 284:1213–1223.
5. Grosshans BL, Ortiz D, Novick P (2006) Rabs and their effectors: achieving specificity in membrane traffic. *Proc Natl Acad Sci USA* 103:11821–11827.
6. Lapierre LA, et al. (2001) Myosin vb is associated with plasma membrane recycling systems. *Mol Biol Cell* 12:1843–1857.
7. Müller T, et al. (2008) MYO5B mutations cause microvillus inclusion disease and disrupt epithelial cell polarity. *Nat Genet* 40:1163–1165.
8. Li BX, Satoh AK, Ready DF (2007) Myosin V, Rab11, and dRip11 direct apical secretion and cellular morphogenesis in developing Drosophila photoreceptors. *J Cell Biol* 177: 659–669.
9. Massarwa R, Schejter ED, Shilo BZ (2009) Apical secretion in epithelial tubes of the Drosophila embryo is directed by the Formin-family protein Diaphanous. *Dev Cell* 16: 877–888.
10. Bryant DM, et al. (2010) A molecular network for de novo generation of the apical surface and lumen. *Nat Cell Biol* 12:1035–1045.
11. Ducharme NA, et al. (2006) MARK2/EMK1/Par-1Balpha phosphorylation of Rab11-family interacting protein 2 is necessary for the timely establishment of polarity in Madin-Darby canine kidney cells. *Mol Biol Cell* 17:3625–3637.
12. Hales CM, Vaerman JP, Goldenring JR (2002) Rab11 family interacting protein 2 associates with Myosin Vb and regulates plasma membrane recycling. *J Biol Chem* 277:50415–50421.
13. Lipatova Z, et al. (2008) Direct interaction between a myosin V motor and the Rab GTPases Ypt31/32 is required for polarized secretion. *Mol Biol Cell* 19:4177–4187.
14. Kenworthy AK (2001) Imaging protein-protein interactions using fluorescence resonance energy transfer microscopy. *Methods* 24:289–296.
15. Ullrich O, Reinsch S, Urbé S, Zerial M, Parton RG (1996) Rab11 regulates recycling through the pericentriolar recycling endosome. *J Cell Biol* 135:913–924.
16. Cramm-Behrens CI, Dienst M, Jacob R (2008) Apical cargo traverses endosomal compartments on the passage to the cell surface. *Traffic* 9:2206–2220.
17. Bryant DM, Mostov KE (2008) From cells to organs: Building polarized tissue. *Nat Rev Mol Cell Biol* 9:887–901.
18. O'Brien LE, Zegers MM, Mostov KE (2002) Opinion: Building epithelial architecture: insights from three-dimensional culture models. *Nat Rev Mol Cell Biol* 3:531–537.
19. Meder D, Shevchenko A, Simons K, Füllekrug J (2005) Gp135/podocalyxin and NHERF-2 participate in the formation of a preapical domain during polarization of MDCK cells. *J Cell Biol* 168:303–313.
20. Ferrari A, Veligodskiy A, Berge U, Lucas MS, Kroschewski R (2008) ROCK-mediated contractility, tight junctions and channels contribute to the conversion of a preapical patch into apical surface during isochoric lumen initiation. *J Cell Sci* 121:3649–3663.
21. Hattula K, et al. (2006) Characterization of the Rab8-specific membrane traffic route linked to protrusion formation. *J Cell Sci* 119:4866–4877.
22. Knödler A, et al. (2010) Coordination of Rab8 and Rab11 in primary ciliogenesis. *Proc Natl Acad Sci USA* 107:6346–6351.
23. Wakabayashi Y, Dutt P, Lippincott-Schwartz J, Arias IM (2005) Rab11a and myosin Vb are required for bile canalicular formation in WIF-B9 cells. *Proc Natl Acad Sci USA* 102:15087–15092.
24. Tzaban S, et al. (2009) The recycling and transcytotic pathways for IgG transport by FcRn are distinct and display an inherent polarity. *J Cell Biol* 185:673–684.
25. Nam KT, et al. (2010) Mature chief cells are cryptic progenitors for metaplasia in the stomach. *Gastroenterology* 139:2028–2037.
26. Ruemmele FM, et al. (2010) Loss-of-function of MYO5B is the main cause of microvillus inclusion disease: 15 novel mutations and a CaCo-2 RNAi cell model. *Hum Mutat* 31:544–551.
27. Sato T, et al. (2007) The Rab8 GTPase regulates apical protein localization in intestinal cells. *Nature* 448:366–369.